

SCIENTIFIC REPORTS



OPEN

Hydroxylamine released by nitrifying microorganisms is a precursor for HONO emission from drying soils

M. Ermel^{1,2,9}, T. Behrendt^{1,3}, R. Oswald¹, B. Derstroff⁴, D. Wu^{1,5,10}, S. Hohlmann¹, C. Stöner⁴, A. Pommerening-Röser⁶, M. Könneke⁷, J. Williams⁴, F. X. Meixner¹, M. O. Andreae^{1,8}, I. Trebs^{1,11} & M. Sörgel¹

Nitrous acid (HONO) is an important precursor of the hydroxyl radical (OH), the atmosphere's primary oxidant. An unknown strong daytime source of HONO is required to explain measurements in ambient air. Emissions from soils are one of the potential sources. Ammonia-oxidizing bacteria (AOB) have been identified as possible producers of these HONO soil emissions. However, the mechanisms for production and release of HONO in soils are not fully understood. In this study, we used a dynamic soil-chamber system to provide direct evidence that gaseous emissions from nitrifying pure cultures contain hydroxylamine (NH₂OH), which is subsequently converted to HONO in a heterogeneous reaction with water vapor on glass bead surfaces. In addition to different AOB species, we found release of HONO also in ammonia-oxidizing archaea (AOA), suggesting that these globally abundant microbes may also contribute to the formation of atmospheric HONO and consequently OH. Since biogenic NH₂OH is formed by diverse organisms, such as AOB, AOA, methane-oxidizing bacteria, heterotrophic nitrifiers, and fungi, we argue that HONO emission from soil is not restricted to the nitrifying bacteria, but is also promoted by nitrifying members of the domains *Archaea* and *Eukarya*.

The photolysis of nitrous acid (HONO) yields the hydroxyl radical (OH), the primary oxidizing agent in the atmosphere, and thereby contributes significantly to the total daily primary OH production (up to 56%¹), particularly in the extratropics. In numerous field studies, measured daytime mixing ratios of HONO have far exceeded model estimates based on known abiotic sources, such as gas phase formation from NO and OH and the heterogeneous disproportionation of NO₂². Consequently, several additional potential sources of HONO have been postulated³. Recently, soil was shown to be an important source of HONO due to the partitioning of nitrous acid between the aqueous phase of soil and the gas phase⁴. This physicochemical approach used the bulk nitrite concentration, the soil water content, and the pH-dependent equilibrium between HONO and nitrite to calculate the concentration of dissolved HONO in the aqueous phase of soil. By examining biological influences, Oswald *et al.*⁵ found strong HONO emissions mainly at low soil water content, with the highest emissions from soils

¹Biogeochemistry Department, Max Planck Institute for Chemistry, P.O. Box 3060, 55020, Mainz, Germany.

²Institute for Inorganic and Analytical Chemistry, Johannes Gutenberg University Mainz, 55128, Mainz, Germany.

³Biogeochemical Processes Department, Max Planck Institute for Biogeochemistry, P.O. Box 10 01 64, 07745, Jena, Germany.

⁴Atmospheric Chemistry Department, Max Planck Institute for Chemistry, P.O. Box 3060, 55020, Mainz, Germany.

⁵Key Laboratory of Agricultural Water Research, Center for Agricultural Resources Research, Institute of Genetic and Developmental Biology, The Chinese Academy of Sciences, 050021, Shijiazhuang, China.

⁶Department of Microbiology and Biotechnology, University of Hamburg, Hamburg, Germany.

⁷MARUM Center for Marine Environmental Sciences and Department of Geoscience, University of Bremen, P.O. Box 330440, 28334, Bremen, Germany.

⁸Scripps Institution of Oceanography, University of California San Diego, San Diego, CA, 92093, USA.

⁹Present address: Messer Industriegase GmbH, Messer-Platz 1, 65812, Bad Soden, Germany.

¹⁰Present address: Key Laboratory of Geographic Information Sciences, Ministry of Education, School of Geographic Sciences, East China Normal University, 200241, Shanghai, China.

¹¹Present address: Environmental Research and Innovation Department, Luxembourg Institute of Science and Technology (LIST), L-4422, Belvaux, Luxembourg.

Correspondence and requests for materials should be addressed to M.S. (email: m.soergel@mpic.de)

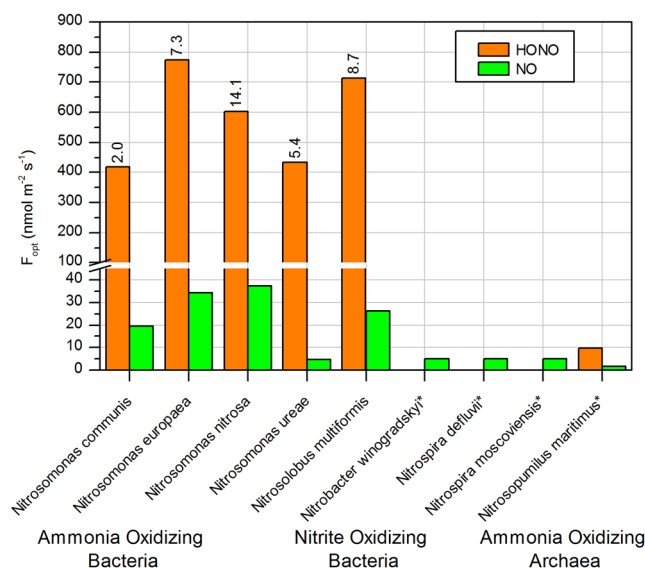


Figure 1. Optimum emissions (F_{opt}) of HONO and NO from the investigated cultures of AOB, NOB and AOA. The cell densities of the pure culture expressed as ATP concentration in $\mu\text{mol l}^{-1}$ are shown by the numbers above the corresponding bars. For NOB and AOA no ATP data is available. Measurements refer to single values as some cultures have been measured repeatedly but at different ATP concentrations (e.g. *N. europaea* emitted 500 to 800 $\text{nmol m}^{-2} \text{s}^{-1}$ for ATP between 2.5 $\mu\text{mol L}^{-1}$ and 10 $\mu\text{mol L}^{-1}$).

at neutral pH, and identified ammonia-oxidizing bacteria (AOB) as a source of HONO. Indeed, *Nitrosomonas europaea* was shown to emit approximately four times more HONO than a sterile control⁵. A recent study successfully combined molecular biological surveys with isotopic measurements, to confirm AOBs as a source of soil emissions. It additionally revealed that more HONO is emitted with increasing soil pH⁶. Soil particle surfaces can be more acidic than the bulk pH, which might explain HONO release at higher bulk soil pH⁷. Interestingly, the optimum pH range of HONO emissions coincides with the optimum pH range for nitrification by AOBs^{8,9}. Therefore, favorable conditions for microbial production (neutral-high pH) appear to be more important than favorable conditions for release (low pH). Despite these recent advances, and the insights in microbial pathways such as NH_2OH oxidation to NO_2^- , the underlying mechanisms that govern the release and the precursor species for non-enzymatic HONO soil emissions remain largely unknown.

An essential and reactive intermediate of nitrification is hydroxylamine (NH_2OH). This species was shown to decompose to N_2O ^{10,11}, which has also been considered as a product of heterogeneous decomposition of HONO/ NO_2^- on soil surfaces^{12,13}. In this study we investigate whether hydroxylamine decomposition can also form HONO. We used a dynamic soil-chamber method¹⁴ to investigate gaseous fluxes of NH_2OH from pure cultures of AOB, nitrite-oxidizing bacteria (NOB), and the ammonia-oxidizing archaeon (AOA), *Nitrosopumilus maritimus*. The liquid culture suspension was applied to glass beads in a petri dish until water holding capacity (WHC) was reached. This setup simulates the soil matrix for the microbes and allows comparison with real soil. Release of gaseous NH_2OH was measured by a Proton-Transfer-Reaction Time-of-Flight Mass Spectrometer (PTR-TOF-MS). The HONO formation from the reaction of gaseous NH_2OH on glass beads was observed with a LOng Path Absorption Photometer (LOPAP).

Results and Discussion

HONO and NO formation were investigated for *Nitrosomonas communis*, *Nitrosomonas europaea*, *Nitrosomonas nitrosa*, *Nitrosomonas ureae*, and *Nitrosolobus multiformis*, which represent all phylogenetic lineages comprising terrestrial and limnic AOB species¹⁵. Additionally, emissions from the NOB species *Nitrobacter winogradskyi*, *Nitrospira defluvii*, and *Nitrospira moscoviensis*, and the AOA *Nitrosopumilus maritimus*, which represents the first characterized AOA¹⁶, were measured. *N. maritimus* has been previously used as model organism to study the mechanism of ammonia oxidation in archaea^{17–19}. Highest emissions of HONO and NO are typically found at a certain gravimetric soil water content (θ_g), termed the optimal water content. These maximal emissions are henceforth denoted as $F_{opt}(\text{HONO})$ and $F_{opt}(\text{NO})$. All measured AOB and AOA strains emitted more HONO than NO (Fig. 1). These results are in good agreement with Oswald *et al.*⁵, who found HONO emissions to be three times higher than NO emissions for a culture of *N. europaea*. In contrast, the NOB, which served as a negative control, emitted only small amounts of NO and no emission of HONO was detectable. This was to be expected from their metabolism, but has not been shown experimentally before. Due to relatively low cell densities and slow growth rates, HONO emission from *N. maritimus* was low (See Fig. 1). Another reason for the low NH_2OH release by AOA may be the nature of the membrane lipids and the thick protein layer surrounding the cells. The membrane consists of a monolayer of tightly packed etherlipids²⁰ and the cell envelope is a hexagonally arrayed single S-layer²¹ that protect the cells from mechanical disruption²². Nevertheless, the measurements provided direct evidence for the potential of AOAs to contribute to HONO emissions. Like their bacterial counterparts,

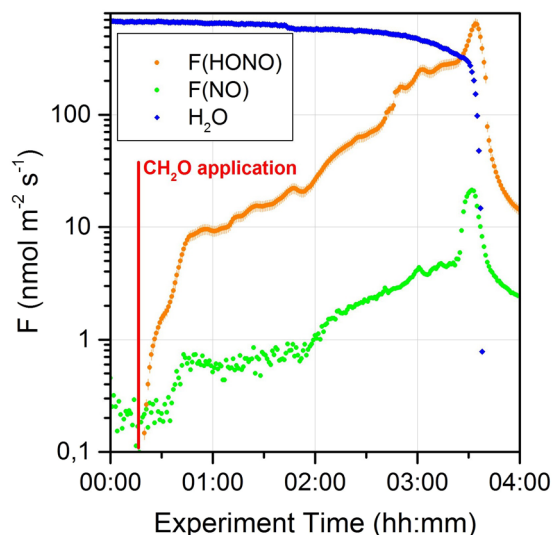


Figure 2. Increased porosity of the cell membrane of *N. europaea* by formaldehyde (CH_2O) causes instantaneous release of HONO and NO. The release of H_2O from the soil sample is represented in arbitrary units.

AOA generate energy by converting ammonia aerobically to nitrite via hydroxylamine¹⁸. The biochemical mechanism of ammonia oxidation in AOA, which is distinct from the bacterial pathway¹⁹, exhibits lower K_M values than those of AOB and enables AOA to thrive at extremely low ammonia concentrations¹⁷. Also in contrast to AOB, some AOA distantly related to *N. maritimus* are able to grow at low pH conditions. The obligate acidophilic AOA, *Nitrosotalea devanaerra*, was isolated from acidic soil and was found to be mainly responsible for autotrophic nitrification under acidic conditions²³. Hence, we argue that globally abundant AOA in soils are likely responsible for biogenic HONO emissions at lower pH conditions than favorable for AOBs, as had been proposed by Scharko *et al.*⁶. This is supported by the results of Oswald *et al.*⁵ who investigated 17 soil samples and found an emission optimum at neutral pH that could be attributed to the activity of AOB. However, a second, smaller maximum was also found at a pH between 5 and 6. Under these conditions, even relatively acid-tolerant AOB are unlikely to be the source of the emissions²⁴, but they appeared to be optimal for growth of the AOA, *N. devanaerra* (pH 5).

The energy metabolisms of both AOB²⁵ and AOA¹⁸ use hydroxylamine (NH_2OH) as an intermediate during the oxidation of ammonia (NH_3) to NO_2^- . Comparison of the genomic inventory suggested that the responsible enzymes for both groups of ammonia-oxidizers differ strongly¹⁹, and so far the biochemical mechanism of the NH_2OH to NO_2^- conversion remains unknown for AOA²⁶. Furthermore, the structures of the enzymes responsible for the reduction of NO_2^- are different for AOA and AOB, and due to the marked differences in the enzymatic pathways of AOB and AOA, we focused our investigations on the metabolites that they have in common. Since we found no correlation between the NO_2^- concentration in the culture solution and the release of HONO from cultures of *N. europaea* (Fig. S2), as would be expected from the partitioning of NO_2^- , we focused on the intermediate, NH_2OH . AOB are able to accumulate NH_2OH to concentrations of up to 0.8 mol l^{-1} ²⁷. In aqueous solutions, NH_2OH is known to be autoxidized to NO_2^- ^{28,29}, providing a potential oxidation pathway to HONO. We added formaldehyde (CH_2O) to a culture of *N. europaea* (Fig. 2) to increase the permeability of the cell membrane, and thereby to trigger the release of NH_2OH and the formation of HONO. Release of HONO and NO occurred immediately after the addition of CH_2O , suggesting that F(HONO) might be linked to the release of the internally accumulated precursor, NH_2OH . In the study of Schmidt and coworkers²⁷, 95% of the NH_2OH inside AOB cells was found to be protein bound. As formaldehyde is known to denature proteins³⁰ the applied CH_2O may not only accelerate the release of internally accumulated NH_2OH but also effectively release the bound NH_2OH from the proteins and therefore accelerate the reaction. The release processes of NH_2OH under natural conditions are still unknown. Stüven and coworkers proposed a pathway for NH_2OH release to the surrounding media to explain NO and N_2O formation by chemodenitrification³¹. The pathway that is utilized by AOB in suspension cultures (no drying out), involves additional electrons that originate from the oxidation of pyruvate or formate and cause an imbalance between ammonia and hydroxylamine oxidation, which leads to a release of NH_2OH ³¹. Furthermore, a recent study³² showed that *N. multiformis* and *N. europaea* released NH_2OH into the medium at measurable amounts, whereas NH_2OH was not detectable in cultures of *N. nitrosa* and *N. communis* grown under the same conditions. Interestingly, in our experiments *N. multiformis* and *N. europaea* showed larger HONO emissions than *N. nitrosa* and *N. communis* (see Fig. 1). Although the measurement of NH_2OH in soils remains difficult due to its reactivity^{12,33}, it is widely accepted that abiotic decomposition of NH_2OH in soils is a non-negligible source of N_2O from soils^{11,12}. To further test if NH_2OH is released by the microorganisms, we measured its concentration in the headspace gas of different soil samples.

A Proton-Transfer-Reaction Time-of-Flight Mass Spectrometer (PTR-TOF-MS) was used to confirm the release of NH_2OH from a sample of an *N. europaea* culture, which had been applied to a glass bead matrix as described previously. In addition, we analyzed the number of membrane-damaged cells by fluorescence

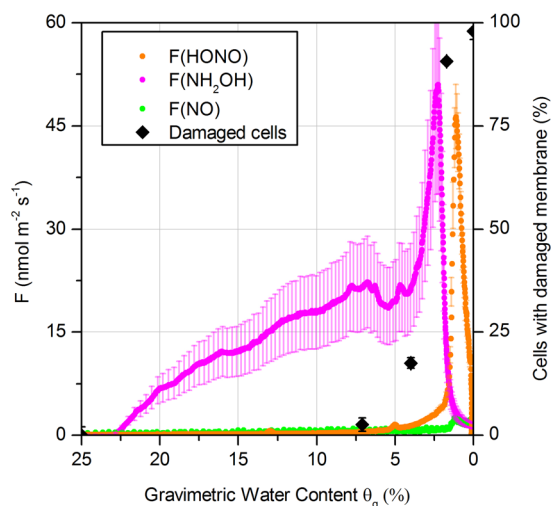


Figure 3. *N. europaea* releases NH_2OH at the same order of magnitude as HONO, but it is emitted at higher gravimetric water content, θ_g , compared to HONO. With decreasing θ_g , the number of cells with membrane damage rises (the time course of the experiment proceeds from left to right). Error bars of damaged cell numbers denote standard deviations ($n = 3$).

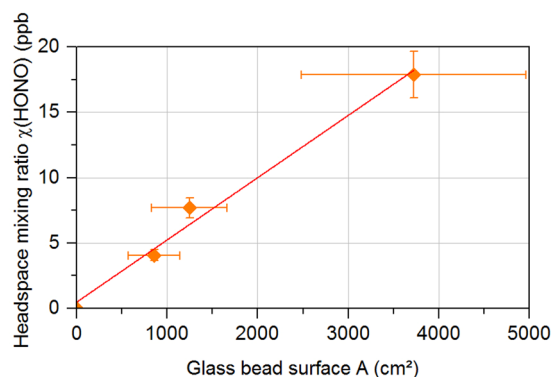
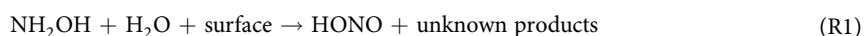


Figure 4. HONO is formed on glass bead surfaces during the surface reaction of NH_2OH (207 ppb) with water vapor ($12.5 \text{ mmol mol}^{-1}$). The point at zero is the value measured without glass beads.

microscopy. As shown in Fig. 3, *N. europaea* released NH_2OH during the experiment. The emission is observed over the entire soil moisture range, and a maximum is found at low θ_g . This pattern differs from that of HONO, which is only released under dry conditions ($\theta_g < 3\%$). Most notably, the release of HONO rises at the same time as the NH_2OH emission fluxes decline sharply. This strongly suggests a conversion of NH_2OH to HONO at low θ_g . The number of cells with a damaged membrane rises substantially at $\theta_g < 7\%$ during the dry-out experiment. This temporal pattern matches with the increased release of NH_2OH and the subsequent HONO formation from the *N. europaea* culture, supporting the hypothesis that accumulated NH_2OH is released and acts as a precursor for the formation of HONO. Although the mechanism is not clear (see above), Fig. 3 shows that NH_2OH is not only released by microorganisms under extreme conditions during dry-out finally causing cell death, but that NH_2OH is released already at $\theta_g < 25\%$. Increasing numbers of damaged cells were only observed for $\theta_g < 7\%$ accompanied with a sharp increase in NH_2OH emissions (from $\sim 20 \text{ nmol m}^{-2} \text{ s}^{-1}$ to about $50 \text{ nmol m}^{-2} \text{ s}^{-1}$), but already starting at a high level.

We further explored the potential conversion of NH_2OH to HONO by investigating the heterogeneous reaction of NH_2OH and water vapor to reflect the conditions at low θ_g . We constructed a NH_2OH permeation source, which supplied the experiment with 207 ppb of gaseous NH_2OH in purified air. This gas stream was humidified and then passed through a cartridge with varying amounts of glass beads (i.e., varying the surface available for reaction) simulating the soil matrix.

A linear relationship between the formed HONO and the glass bead surface area was found (Fig. 4) for constant levels of gaseous NH_2OH . Therefore, the reaction can be summarized as:



The highest conversion yield of NH_2OH to HONO was 8.6%, with a contact time of ~ 3 s between the molecules and a glass bead surface of 3600 cm^2 . Under dry conditions (dew point of about -30°C), no formation of HONO was observed demonstrating that water vapor is necessary for the reaction. Moreover, a significant gas phase reaction of NH_2OH and water vapor was not found (measurement without glass beads Fig. 4). Our results therefore demonstrate that HONO is formed from NH_2OH on surfaces at low humidity conditions. This heterogeneous reaction may explain why HONO emissions are restricted to low θ_g ($< 3\%$; see Fig. 3), as the glass bead surface is free of liquid water films, in which the slow autoxidation of NH_2OH ^{28,29} occurs, only under these dry conditions and is only then available for the surface reaction R1.

The analysis of four different soil samples did not show any measurable NH_2OH emissions. It is possible that there was a small NH_2OH release, which we were unable to detect because of the interference from the minor isotopomer of methanol ($^{13}\text{CH}_3\text{OH}$), as both signals overlap and are within the noise level of the instrument. However, we consider it more likely that the lack of observable NH_2OH emission is explained by its efficient conversion to HONO in natural soils, since the specific surface area of natural soils ($\sim 10^3\text{--}10^6\text{ cm}^2\text{ g}^{-1}$) is significantly greater than that of the glass beads ($59.6\text{ cm}^2\text{ g}^{-1}$)^{34,35}. Our results support the assumption made by previous authors that NH_2OH could not be detected in soils due to its reactivity^{12,28}. By linearly extrapolating the relationship between surface area and conversion yield from our experiments (Fig. 4), a complete conversion can be expected under our experimental conditions (i.e., ~ 200 ppb NH_2OH in air, residence time 3 sec) at around $4 \times 10^4\text{ cm}^2$, corresponding to only 0.4 g of a soil with a medium specific surface area of $10^5\text{ cm}^2\text{ g}^{-1}$. Furthermore, the decomposition of NH_2OH and $\text{HONO}/\text{NO}_2^-$ is thought to be catalyzed by metal oxides^{11,12,36}, many of which are present in soil. Consequently, the release of HONO by soil is partly attributable to NH_2OH that has been converted within the soil matrix over the prolonged reaction time and high surface area. Therefore, NH_2OH might also contribute indirectly to NO pulses observed during rewetting of the soils as they have been attributed to decomposition of $\text{HONO}/\text{NO}_2^-$, which had accumulated in the soil during dry-out (with a potential contribution from NH_2OH decomposition), in their initial phase³⁷.

Conclusions

A new formation pathway for HONO in dry soils was identified. Our study reveals that NH_2OH released by microorganisms, especially under the conditions of increased permeability of cell membranes or cell death during dry-out, is decomposed in soils and yields HONO by a heterogeneous reaction on soil particles involving NH_2OH and H_2O . This reaction may explain a substantial fraction of the HONO emission observed at low soil water content. Our results show that these biogenic HONO emissions are not restricted to AOB, but that also AOA are contributing to the release of this important trace gas.

Our results suggest that all organisms that produce NH_2OH at some stage in their metabolism are potential contributors to the formation of HONO. Within the nitrogen cycle, NH_2OH is also produced during the heterotrophic nitrification from bacteria of different genera³⁸. Methane-oxidizing bacteria are another group of bacteria that is capable of producing NH_2OH ³⁹, and even eukaryotic species such as the fungus *Aspergillus flavus* have been shown to be a source⁴⁰. Hence, the capability to contribute to HONO formation in soils is present in all three domains of life, including bacteria, archaea, and eukaryotes.

Methods

We used the dynamic chamber method¹⁴ (and below) to investigate gaseous fluxes from pure cultures of AOB, nitrite-oxidizing bacteria (NOB) and the ammonia-oxidizing archaeon (AOA), *Nitrosopumilus maritimus*. Liquid culture suspension from pure cultures of AOB, nitrite-oxidizing bacteria (NOB) and the ammonia-oxidizing archaeon (AOA), *Nitrosopumilus maritimus*, were applied to soda lime glass beads (0.25–0.50 mm diameter, Carl Roth, Germany) in a petri dish until water holding capacity (WHC) was reached. This setup simulates the soil matrix for the microbes and allows comparison with real soil. The petri dish containing the sample was subsequently placed into the dynamic chamber, which was flushed with purified dry air (free from NO , NO_2 , O_3 , H_2O , VOCs, NH_2OH , and HONO). Due to the flow of dry air over the sample, it is gradually dried out in the course of an experiment. The cell density of a culture was characterized by the content of adenosine 5'-triphosphate (ATP) ($\mu\text{mol l}^{-1}$), which correlated well with the microscopically derived cell density (Fig. S1). Prior to each experiment, the cell density was determined and found to be between 2 to $20\ \mu\text{mol l}^{-1}$ ATP (data not available for NOB and AOA experiments). Significant growth of the culture during an experiment can be excluded, as typical doubling times of AOB are between 12 and 20 hours⁴¹, and ≥ 21 hours for the investigated AOA¹⁶, whereas the duration of an experiment was 6 to 10 hours.

Dynamic Chamber. A chamber coated with polyfluoroethylene (PFE) foil with a volume of 0.008 m^3 was flushed at a flow rate of $1 \cdot 10^{-4}\text{ m}^3\text{ s}^{-1}$ with dry purified air (Figure S3). Air purification was achieved as follows: the air was passed through a membrane dryer combined with a filter for compressed air (Clearpoint and Drypoint M from BEKO Deutschland GmbH, Germany). In a second step, a UV lamp (OG-1, Ultra-Violet Products Ltd, USA) was used to photolyze HONO to NO and OH. A pure-air generator (PAG 003, ECOPHYSICS, Switzerland) was used to remove further trace gases such as HONO, NO_x , O_3 , hydrocarbons, and water vapor. To prevent any traces of reactive nitrogen gases from entering the system, a cartridge filled with Purafil (Headline Filters, Germany) was installed after the pure air generator. To ensure sterile conditions in the chamber, the inlet was equipped with a sterile air filter (MILEX[®]-FG Vent Filter $0.2\ \mu\text{m}$, 50 mm diameter, Millipore, France). NO_x ($\text{NO} + \text{NO}_2$) was measured at the outlet of the chamber by a chemiluminescence analyzer (CLD 780TR, ECOPHYSICS, Switzerland, limit of detection (LOD): $\text{LOD}_{\text{NO}} \approx 35\text{ ppt}$ and $\text{LOD}_{\text{NO}_2} \approx 120\text{ ppt}$), where NO_2 was detected after conversion to NO by a blue light converter (Air Quality Design, Inc., Co, USA). A UV-absorption analyzer (Model 49i, Thermo Electron Corporation, USA; $\text{LOD} \approx 0.5\text{ ppb}$) was used to measure O_3 levels to ensure that no outside air was entering the system. The water vapor difference between the inlet and outlet of

the chamber was measured with an infrared gas analyzer (LI-7000, Li-Cor Biosciences GmbH, Germany). To avoid any wall losses, the long path absorption photometer (LOPAP) (QUMA Elektronik & Analytik GmbH, Wuppertal, LOD \approx 5 ppt) was directly connected to the chamber to measure HONO. The chamber and the LOPAP sampling unit were placed in a temperature-controlled cabinet. Data were acquired by a CR3000 data logger (Campbell Scientific, Inc., USA) every 60 s.

NH₂OH measurements. Gaseous hydroxylamine (NH₂OH) was determined with a commercial PTR-TOF-MS (Proton-Transfer-Reaction Time-of-Flight Mass Spectrometer, Ionicon Analytik GmbH, Innsbruck, Austria)⁴². This measurement technique utilizes the protonation of molecules with a proton affinity higher than water by H₃O⁺ ions that are generated in a hollow cathode discharge. NH₂OH has a proton affinity of 803 kJ mol⁻¹⁴³, while the value for water is 691 kJ mol⁻¹⁴⁴. All protonated molecular ions are accelerated by an electrical field to the same kinetic energy such that the resultant velocity of the ions depends on the mass-to-charge ratio. Hence, the velocity is measured as the time-of-flight, from which the mass-to-charge ratio can be calculated⁴⁵. The mass resolution was approximately 3700 m/ Δ m and NH₂OH was measured at mass 34.029. It should be noted that the ¹³C isotope of methanol at mass 34.037, which represents 1% of the methanol signal, potentially interferes with ambient NH₂OH measurements from soil, but not with those from the cultures. For the experiment with a pure culture of *N. europaea*, NH₂OH was in large excess over methanol. The instrument was operated with a drift pressure of 2.20 hPa (E/N 140 Td) and a drift voltage of 600 V. 1,3,5-trichlorobenzene was used as internal standard for mass scale calibration. Data post-processing and analysis was performed by using the program “PTR-TOF DATA ANALYZER”⁴⁶. The NH₂OH measurements were made with the chamber system described by Behrendt *et al.*⁴⁷. The effect of wall losses was minimized by using the same inlet tube length for calibration and measurement. The instrument was calibrated for gas phase NH₂OH using a custom built sublimation unit with NH₂OH purified by the method of Chang *et al.*⁴⁸. NH₂OH was exposed to a nitrogen gas flow and the concentration was determined gravimetrically. The PTR-TOF-MS was calibrated with a NH₂OH mixing ratio of 893.8 ppb. Since the measured mixing ratios of NH₂OH were lower (0–230 ppb) than the single-point calibration value, we assume a systematic error of 30%, in contrast to compounds calibrated with pressurized gas standards, which typically have an overall uncertainty of about 10%. The calculated detection limit (3 σ of the noise) was about 15 ppt. For the surface reaction experiment with glass beads, the gas flow from the NH₂OH source (745 ppb) was diluted with humidified air (12.5 mmol mol⁻¹ H₂O) to a mixing ratio of 207 ppb NH₂OH and directly passed through a cartridge filled with the glass beads. The HONO produced from wall reactions inside the system (without glass beads) has been subtracted.

The measurement of NH₂OH by any technique requiring tubing connections is challenging, because this molecule has a high affinity to adsorb on tubing walls due to its polarity. The possibility that the maximum F(NH₂OH) observed in Fig. 3 was related to a desorption of NH₂OH from the tubing, caused by the decreasing humidity, is unlikely, since similarly soluble molecules, e.g., methanol, did not show such effects. Based on humidity dependent calibrations of multiple volatile organic compound standards, the peak of NH₂OH shown in Fig. 3 is far too large to be explained by instrumental sensitivity changes associated with humidity. Extensive calibrations with the analogous species methanol between 25–80% RH have shown variations of between 10–20% in sensitivity, whereas many compounds such as isoprene show no humidity dependence at all.

Further information on cultivation of microorganisms, soil sampling and analysis, measurement of microorganisms and soil samples, and flux calculations can be found in the supplementary information.

Data availability. Data are available on request from m.soergel@mpic.de.

References

- Ren, X. *et al.* OH and HO₂ Chemistry in the urban atmosphere of New York City. *Atmos. Environ.* **37**, 3639–3651 [https://doi.org/10.1016/S1352-2310\(03\)00459-X](https://doi.org/10.1016/S1352-2310(03)00459-X) (2003).
- Sörgel, M. *et al.* Quantification of the unknown HONO daytime source and its relation to NO₂. *Atmos. Chem. Phys.* **11**, 10433–10447, <https://doi.org/10.5194/acp-11-10433-2011> (2011).
- Kleffmann, J. Daytime sources of nitrous acid (HONO) in the atmospheric boundary layer. *Chemphyschem* **8**, 1137–1144, <https://doi.org/10.1002/cphc.200700016> (2007).
- Su, H. *et al.* Soil nitrite as a source of atmospheric HONO and OH radicals. *Science* **333**, 1616–1618, <https://doi.org/10.1126/science.1207687> (2011).
- Oswald, R. *et al.* HONO emissions from soil bacteria as a major source of atmospheric reactive nitrogen. *Science* **341**, 1233–1235, <https://doi.org/10.1126/science.1242266> (2013).
- Scharko, N. K. *et al.* Combined Flux Chamber and Genomics Approach Links Nitrous Acid Emissions to Ammonia Oxidizing Bacteria and Archaea in Urban and Agricultural Soil. *Environ. Sci. Technol.* **49**, 13825–13834, <https://doi.org/10.1021/acs.est.5b00838> (2015).
- Donaldson, M. A., Bish, D. L. & Raff, J. D. Soil surface acidity plays a determining role in the atmospheric-terrestrial exchange of nitrous acid. *P. Natl. Acad. Sci. USA* **111**, 18472–18477, <https://doi.org/10.1073/pnas.1418545112> (2014).
- Park, S., Bae, W., Chung, J. & Baek, S.-C. Empirical model of the pH dependence of the maximum specific nitrification rate. *Process Biochem.* **42**, 1671–1676, <https://doi.org/10.1016/j.procbio.2007.09.010> (2007).
- Nicol, G. W., Leininger, S., Schleper, C. & Prosser, J. I. The influence of soil pH on the diversity, abundance and transcriptional activity of ammonia oxidizing archaea and bacteria. *Environ. Microbiol.* **10**, 2966–2978, <https://doi.org/10.1111/j.1462-2920.2008.01701.x> (2008).
- Van Cleemput, O. & Samater, A. H. Nitrite in soils: accumulation and role in the formation of gaseous N compounds. *Fert. Res.* **45**, 81–89 (1996).
- Bremner, J. M. Sources of nitrous oxide in soils. *Nutr. Cycl. Agroecosys.* **49**, 7–16 (1997).
- Heil, A., Vereecken, H. & Brüggemann, N. A review of chemical reactions of nitrification intermediates and their role in nitrogen cycling and nitrogen trace gas formation in soil. *Eur. J. Soil Sci* **67**, 23–39 (2016).
- Donaldson, M. A., Berke, A. E. & Raff, J. D. Uptake of gas phase nitrous acid onto boundary layer soil surfaces. *Environ. Sci. Technol.* **48**, 375–383 (2014).

14. Breuninger, C., Oswald, R., Kesselmeier, J. & Meixner, F. X. The dynamic chamber method: trace gas exchange fluxes (NO, NO₂, O₃) between plants and the atmosphere in the laboratory and in the field. *Atmos. Meas. Tech.* **5**, 955–989, <https://doi.org/10.5194/amt-5-955-2012> (2012).
15. Koops, H. P. & Pommerening-Röser, A. Distribution and ecophysiology of the nitrifying bacteria emphasizing cultured species. *FEMS Microbiol. Ecol.* **37**, 1–9, <https://doi.org/10.1111/j.1574-6941.2001.tb00847.x> (2001).
16. Könneke, M. *et al.* Isolation of an autotrophic ammonia-oxidizing marine archaeon. *Nature* **437**, 543–546, <https://doi.org/10.1038/Nature03911> (2005).
17. Martens-Habbena, W., Berube, P. M., Urakawa, H., de la Torre, J. R. & Stahl, D. A. Ammonia oxidation kinetics determine niche separation of nitrifying Archaea and Bacteria. *Nature* **461**, 976–979 (2009).
18. Vajrjala, N. *et al.* Hydroxylamine as an intermediate in ammonia oxidation by globally abundant marine archaea. *P. Natl. Acad. Sci. USA* **110**, 1006–1011, <https://doi.org/10.1073/pnas.1214272110> (2013).
19. Walker *et al.* Nitrosopumilus maritimus genome reveals unique mechanisms for nitrification and autotrophy in globally distributed marine crenarchaea. *P. Natl. Acad. Sci. USA* **107**, 8818–8823 (2010).
20. Elling, F. J. *et al.* Chemotaxonomic characterisation of the thaumarchaeal lipidome. *Envi. Microbiol.* **19**, 2681–2700, <https://doi.org/10.1111/1462-2920.13759> (2017).
21. Quin, W. *et al.* Nitrosopumilus maritimus gen. nov., sp. nov., Nitrosopumilus cobalaminigenes sp. nov., Nitrosopumilus oxycliniae sp. nov., and Nitrosopumilus ureiphilus sp. nov., four marine ammonia-oxidizing archaea of the phylum Thaumarchaeota, *Int. J. Syst. Evol. Micro.*, <https://doi.org/10.1099/ijsem.0.002416> (2017).
22. Könneke, M. Stoffwechsel mariner Ammoniakoxidierender Archaeen, *Biospektrum* **21**, <https://doi.org/10.1007/s12268-015-0570-2>, 267–269 (2015).
23. Lehtovirta-Morley, L. E., Stoecker, K., Vilcinskas, A., Prosser, J. I. & Nicol, G. W. Cultivation of an obligate acidophilic ammonia oxidizer from a nitrifying acid soil. *P. Natl. Acad. Sci. USA* **108**, 15892–15897, <https://doi.org/10.1073/pnas.1107196108> (2011).
24. Pommerening-Röser, A. & Koops, H. P. Environmental pH as an important factor for the distribution of urease positive ammonia-oxidizing bacteria. *Microbiol. Res.* **160**, 27–35, <https://doi.org/10.1016/j.micres.2004.09.006> (2005).
25. Koops, H.-P., Purkhold, U., Pommerening-Röser, A., Timmermann, G. & Wagner, M. The Lithoautotrophic Ammonia-Oxidizing Bacteria: *The Prokaryotes* Vol. 5, Ch.3.2.12 (Springer, New York, 2006).
26. Stahl, D. A. & de la Torre, J. R. Physiology and Diversity of Ammonia-Oxidizing Archaea. *Annu. Rev. Microbiol.* **66**, 83–101, <https://doi.org/10.1146/annurev-micro-092611-150128> (2012).
27. Schmidt, I., Look, C., Bock, E. & Jetten, M. S. M. Ammonium and hydroxylamine uptake and accumulation in *Nitrosomonas*. *Microbiology* **150**, 1405–1412, <https://doi.org/10.1099/mic.0.26719-0> (2004).
28. Moews, P. C. & Audrieth, L. F. The autoxidation of hydroxylamine. *J. Inorg. Nucl. Chem.* **1**, 242–246 (1959).
29. Hughes, M. N. & Nicklin, H. G. Autoxidation of hydroxylamine in alkaline solutions. *J. Chem. Soc. A*, 164–168, <https://doi.org/10.1039/j19710000164> (1971).
30. Mason, J. T. & O’Leary, T. J. Effects of formaldehyd fixation on protein secondary structure: A colorimetric and infrared spectroscopic investigation. *J. Histochem. Cytochem.* **39**, 225–229 (1991).
31. Stüven, R., Vollmer, M. & Bock, E. The impact of organic matter on nitric oxide formation by *Nitrosomonas europaea*. *Archives of Microbiology* **158**, 439–443 (1992).
32. Liu *et al.* Abiotic Conversion of Extracellular NH₂OH Contributes to N₂O Emission during Ammonia Oxidation. *Envi. Sci. Technol.* **51**, 13122–13132, <https://doi.org/10.1021/acs.est.7b02360> (2017).
33. Liu, S., Vereecken, H. & Brüggemann, N. A highly sensitive method for the determination of hydroxylamine in soils. *Geoderma*, **232–234**, 117–122 <https://doi.org/10.1016/j.geoderma.2014.05.006> (2014).
34. Petersen, L. W., Moldrup, P., Jacobsen, O. H. & Rolston, D. E. Relations between surface area and soil physical and chemical properties. *Soil Sci.* **161**, 9–21 (1991).
35. Macht, F., Eusterhues, K., Pronk, G. J. & Totsche, K. U. Specific surface area of clay minerals: Comparison between atomic force microscopy measurements and bulk-gas (N₂) and -liquid (EGME) adsorption methods. *Appl. Clay Sci.* **53**, 20–26 (2011).
36. Liu, S., Berns, A. E., Vereecken, H., Wu, D. & Brüggemann, N. Interactive effects of MnO₂, organic matter and pH on abiotic formation of N₂O from hydroxylamine in artificial soil mixtures, *Scientific Repots* **7**, <https://doi.org/10.1038/srep39590> (2017a).
37. Homyak *et al.* Aridity and plant uptake interact to make dryland soils hotspots for nitric oxide (NO) emissions. *Proc Natl Acad Sci USA* **113**, E2608–E2616 (2016).
38. Otte, S., Schalk, J., Kuenen, J. G. & Jetten, M. S. M. Hydroxylamine oxidation and subsequent nitrous oxide production by the heterotrophic ammonia oxidizer *Alcaligenes faecalis*. *Appl. Microbiol. Biot.* **51**, 255–261, <https://doi.org/10.1007/s002530051390> (1999).
39. Stein, L. Y. & Klotz, M. G. Nitrifying and denitrifying pathways of methanotrophic bacteria. *Biochem. Soc. Trans.* **39**, 1826–1831 (2011).
40. Marshall, K. C. & Alexander, M. Nitrification by *Aspergillus Flavus*. *J. Bacteriol.* **83**, 572–578 (1962).
41. Belsler, L. W. & Schmidt, E. L. Growth and Oxidation-Kinetics of 3 Genera of Ammonia Oxidizing Nitrifiers. *Fems Microbiol. Lett.* **7**, 213–216 (1980).
42. Graus, M., Müller, M. & Hansel, A. High resolution PTR-TOF: quantification and formula confirmation of VOC in real time. *J. Am. Soc. Mass. Spectr.* **21**, 1037–1044 (2010).
43. Jolly, W. L. *Modern Inorganic Chemistry*. (McGraw-Hill, New York, 1991).
44. Linstrom, P. J. M., W.G. (ed. Mallard, P. J. & Linstrom, W. G.) (National Institute of Standards and Technology, Gaithersburg MD, 20899, <http://webbook.nist.gov>, 2009).
45. Williams, J. *Analytical Techniques for Atmospheric Measurement: Mass Spectrometric Methods for Atmospheric Trace Gases Ch. 5* (Blackwell Publishing, Oxford, UK, 2006).
46. Müller, M., Mikoviny, T., Jud, W., D’Anna, B. & Wisthaler, A. A new software tool for the analysis of high resolution PTR-TOF mass spectra. *Chemometr. Intell. Lab.* **127**, 158–165 (2013).
47. Behrendt, T. *et al.* Characterisation of NO production and consumption: new insights by an improved laboratory dynamic chamber technique. *Biogeosciences* **11**, 5463–5492, <https://doi.org/10.5194/bg-11-5463-2014> (2014).
48. Chang, Y. *et al.* Paper-like N-doped graphene films prepared by hydroxylamine diffusion induced assembly and their ultrahigh-rate capacitive properties. *Electrochim. Acta* **115**, 461–470, <https://doi.org/10.1016/j.electacta.2013.10.203> (2014).

Acknowledgements

This project was funded by the Max Planck Society and the Max Planck Graduate Center with the Johannes Gutenberg-Universität Mainz (MPGC). M. Könneke was supported by a DFG Heisenberg Fellowship (KO 3651/3-1). We are grateful to M. Welling, T. Klüpfel, and P. Stella for supporting the experiments. We thank E. Spieck from the University of Hamburg for providing the cultures of nitrite-oxidizing bacteria.

Author Contributions

M.E., T.B., R.O., I.T., M.S. and A. P.-R. designed the experiments. M.E. performed the experiments. S.H. and D.W. supported the experiments. B.D., M.E., C.S. and J.W. performed the NH_2OH measurements. M. K. contributed to the AOA measurements and provided the AOA culture. M.E., F.X.M., I.T., M. K., M.S. and M.O.A. wrote the paper. All authors reviewed the paper.

Additional Information

Supplementary information accompanies this paper at <https://doi.org/10.1038/s41598-018-20170-1>.

Competing Interests: The authors declare that they have no competing interests.

Publisher's note: Springer Nature remains neutral with regard to jurisdictional claims in published maps and institutional affiliations.



Open Access This article is licensed under a Creative Commons Attribution 4.0 International License, which permits use, sharing, adaptation, distribution and reproduction in any medium or format, as long as you give appropriate credit to the original author(s) and the source, provide a link to the Creative Commons license, and indicate if changes were made. The images or other third party material in this article are included in the article's Creative Commons license, unless indicated otherwise in a credit line to the material. If material is not included in the article's Creative Commons license and your intended use is not permitted by statutory regulation or exceeds the permitted use, you will need to obtain permission directly from the copyright holder. To view a copy of this license, visit <http://creativecommons.org/licenses/by/4.0/>.

© The Author(s) 2018